VIP-MAN: AN IMAGE-BASED WHOLE-BODY ADULT MALE MODEL CONSTRUCTED FROM COLOR PHOTOGRAPHS OF THE VISIBLE HUMAN PROJECT FOR MULTI-PARTICLE MONTE CARLO CALCULATIONS

X. G. Xu,*† T. C. Chao,* and A. Bozkurt*

Abstract-**Human anatomical models** have been indispensable to radiation protection dosimetry using Monte Carlo calculations. Existing MIRD-based mathematical models are easy to compute and standardize, but they are simplified and crude compared to human anatomy. This article describes the development of an image-based whole-body model, called VIP-Man, using transversal color photographic images obtained from the National Library of Medicine's Visible Human Project for Monte Carlo organ dose calculations involving photons, electron, neutrons, and protons. As the first of a series of papers on dose calculations based on VIP-Man, this article provides detailed information about how to construct an image-based model, as well as how to adopt it into well-tested Monte Carlo codes, EGS4, MCNP4B, and MCNPX.
Health Phys. 78(5):476–486; 2000

Key words: Monte Carlo; modeling, dose assessment; imaging; dose, internal

INTRODUCTION

Dose assessment in health physics (radiation protection) relies largely on a few sets of basic organ dosimetric quantities. For example, the fluence-to-dose-equivalent conversion factors are the basis for facility shielding design and for calculating dose to a worker/patient exposed to radiation external to the body (ICRU 1998). For assessing dose equivalent to target organs due to radionuclides internally deposited in the source organ(s) following an accidental intake or a nuclear medicine procedure, the specific absorbed fractions (SAFs) or the specific effective energies (SEEs) are used (Snyder et al. 1978; ICRP 1979, 1990). The whole-body risk can then

* Nuclear Engineering and Engineering Physics Programs, NES Building, Tibbits Avenue, Rensselaer Polytechnic Institute, Troy, NY 12180; † Medical Physics Division, Department of Radiation Oncology, Albany Medical College, 47 New Scotland Avenue, Albany, NY 12208.
For correspondence or reprints contact: X. G. Xu, Nuclear Engineering and Engineering Physics Programs, NES Building, Tibbits Avenue, Rensselaer Polytechnic Institute, Troy, NY 12180, or email at xug2@rpi.edu.

be assessed by using ICRP methodologies for effective dose or effective dose equivalent (ICRP 1990; U.S. NRC 1991). The conversion factors and SAFs have been pre-determined using human anatomical models and Monte Carlo calculations. The computational procedures involve careful specification of the human body and the irradiation conditions. Radiation transport and energy deposition in the body are taken care of by a Monte Carlo code. It is apparent that the accuracy of these quantities (and others derived from them) depends upon the body modeling, radiation environment modeling, and the Monte Carlo treatment. Over the years, health physics dosimetry has been incrementally improved by adopting more realistic body models and better Monte Carlo techniques, This article is about the latest effort to revolutionize the way the models are developed and adopted for Monte Carlo calculations.

Existing mathematical models

Early models representing the human body were mostly homogeneous slabs, cylinders, and spheres. The first heterogeneous anthropomorphic model was devised at Oak Ridge National Laboratory for the Medical Internal Radiation Dose (MIRD) Committee of The Society of Nuclear Medicine (Snyder et al. 1969, 1978). This model, known as MIRD Phantom, was based on the concept of the "Reference Man" for radiation protection purposes, although it was recognized that variation among individuals could be significant (ICRP 1975). Reference Man was originally defined as being a 20–30-y-old Caucasian, weighing 70 kg and 170 cm in height. The original MIRD phantom was analytically described in three principal sections: an elliptical cylinder representing the arm, torso, and hips; a truncated elliptical cone representing the legs and feet; and an elliptical cylinder representing the head and neck. The mathematical descriptions of the organs were formulated based on descriptive and schematic materials from general anatomy references. The goal was to make the mathematical equations simple, thus minimizing computation time (Snyder et al. 1978; ICRP 1987, 1996). More than 40 organs and tissues were specified, with basically three media of distinct densities: bone, soft tissue, and lung. Later improvements at Oak Ridge National Laboratory

have led to a "family" of models having both sexes at various ages (Cristy and Eckerman 1987). Others have developed similar models known as the "Adam" and "Eva" (Kramer et al. 1982). One of the most recent improvements is a newly revised head and brain model (Bouchet et al. 1996). These MIRD-based models have served practically as the "standard" to the health physics community. Fig. 1 shows exterior and cut-away views of the mathematical models. Several groups of researchers worldwide have used these MIRD-based mathematical models extensively, with different Monte Carlo computer codes, to calculate internal and external organ doses for a variety of health physics applications involving photon, electron, neutron, and proton sources. For a comprehensive listing of papers and discussions, the readers are referred to ICRU Report 48 (1992) and ICRP Publication 74 (1996). For more than two decades, MIRD-based mathematical models allowed the radiation protection community to gain important insights into the distribution of organ doses that were difficult or impossible to study with physical phantoms.

It is clear, however, that the human anatomy is too complex to be realistically modeled with a limited set of equations. As such, many anatomical details in the mathematical models had to be compromised. In spite of the effort to develop more complicated mathematical models, they remain simplified and crude. For instance, the skeleton in the MIRD mathematical model does not resemble a human, and the radiosensitive red bone marrow is not represented. Many researchers have begun to realize that today's computers are so powerful that it is technically *no longer* necessary to limit the geometry representation to overly simplified shapes. The medical community had already started using advanced imaging techniques, such as Computed Tomography (CT) and Magnetic Resonance Imaging (MRI), to study patient-specific anatomy. These new technologies suggest new types of body models for health physics dosimetry that are image-based and realistic.

Image-based models

3-D medical imaging techniques, such as CT and MRI, have advanced remarkably, allowing us to easily visualize the internal structures of the body and to store the images in versatile digital formats. In the past few years, the radiotherapy community (e.g., the Peregrine Project) has begun to use Monte Carlo techniques with patient CT images for clinical treatment dose optimization (Hartmann Siantar et al. 1997). Compared to the medical community, however, health physicists face at least the following unique and intractable technical challenges: 1) Whole-body models are needed for most health physics applications, but medical images are taken only for a portion of the body (CT procedures expose the patients to intense x rays and MRI is time-consuming); 2) A large amount of internal organs/tissues have to be identified and segmented for organ dose calculations in health physics, while, in radiotherapy, only the tumor volume needs to be specified; 3) The size of a whole-body model can be potentially too big for computers and Monte Carlo codes to handle; and 4) Health physics dosimetry involves photons, electrons, neutrons, and protons, but the majority of the clinical radiotherapy procedures involve only photon/electron beams or seeds (a few centers also involve neutron or proton beams).

Because of these issues, only a few groups have successfully constructed image-based whole-body models (e.g., Zubal et al. 1994; Jones 1997; Hickman and Firpo 1997; Petoussi-Henβ and Zankl 1998). However, these models have some of the following shortcomings:
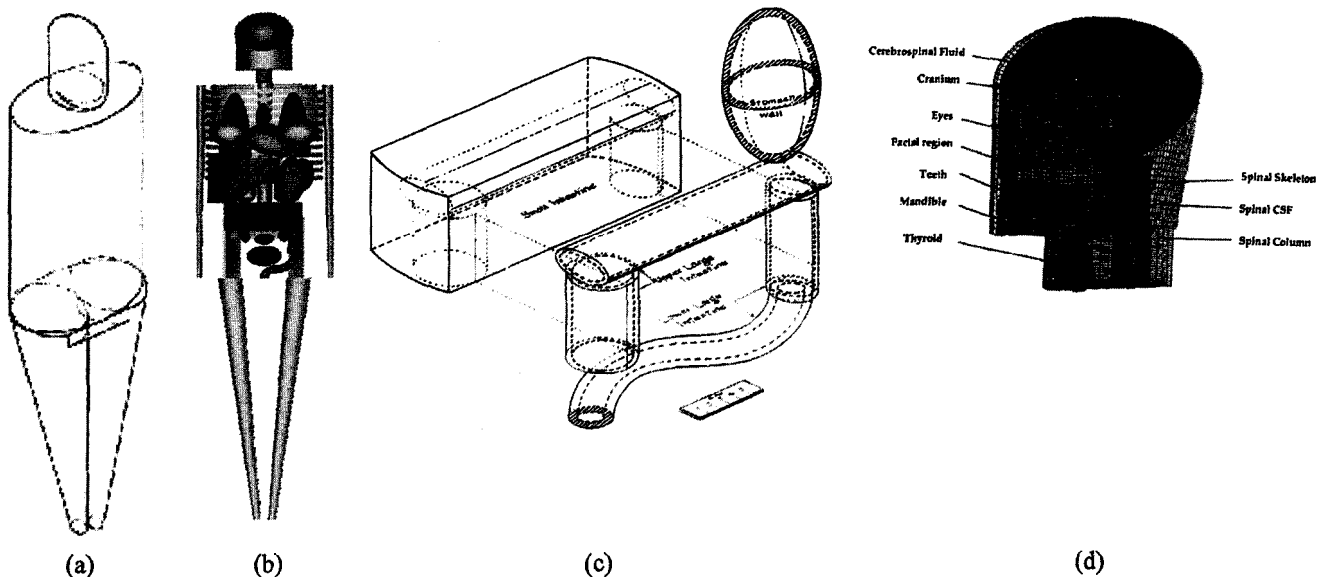

Fig. 1. MIRD-based mathematical adult male model showing (a) exterior view; (b) skeleton and internal organs; (c) detailed GI track; and (d) a recently revised MIRD head and brain model.

1) Not good enough resolutions for small anatomical structures; 2) Not whole body; or 3) No segmentation done. So far all calculations have been only related to photons, and there are practically no results on electron, proton, or neutron sources.

Monte Carlo methods

Analytical calculations for the transport of the radiation through media can be performed only in very simple geometries and under severe approximations. Monte Carlo method, which is based on the first principles, provides the only practical way of performing accurate calculations of 3-D dose distributions from particle interactions in a complex target such as the human body. The earliest use of a Monte Carlo simulation technique was around 1873 (Hammersley and Handscomb 1964). The real development and application of the technique, however, stemmed from work on the atomic bomb during World War II by von Neumann, Ulam, and Fermi. Neumann coined the term "Monte Carlo" to reflect the idea that a conceptual roulette wheel could be employed to select the random nuclear processes. Today, a computer-generated random number between 0 and 1 is used for this purpose. The random number determines which interaction will occur by comparing probabilities (i.e., cross sections) of each interaction. The process is repeated and a particle is tracked in the target until it deposits all its energy or escapes. When a large number of particles (usually several million) are studied this way, the results accurately predict the physical processes that may be experimentally determined. Validation of a code must be done before the code may be used for calculations.

The widespread acceptance of computational models in radiation dosimetry was made possible by the availability of well-validated and maintained Monte Carlo codes and very fast personal computers since the late 1980's. Among all the Monte Carlo codes, there are four general purpose codes that have been widely used in the United States and elsewhere: 1) **EGS4**, originally developed at Stanford Linear Accelerator Center, is well known for its detailed physics treatment involving electron-gamma showers (Nelson et al. 1985). Electron transport algorithms, such as the PRESTA, make EGS4 one of the most sophisticated and efficient photon/electron codes ever developed; 2) **MCNP,** originated from Los Alamos National Laboratory, has the capability to transport photons, neutrons, and in the recent version 4B, also the electrons (Hendricks 1997). MCNP4B has a generalized input capability allowing a user to model a variety of source and detector conditions without having to modify the source code itself. The "lattice structure" feature facilitates the definition of repeated "cells." However, MCNP is not as efficient as EGS4 in tracking particles in a target that has a very large amount of divided regions; 3) **LAHET** is a code for the transport and interaction of nucleons, pions, muons, light ions, and anti-nucleons in complex geometry (Prael and Lichtenstein 1989). The code handles geometry input and the

tracking of the particles the same way as MCNP. For neutron interactions above a cutoff energy (20 MeV), the code uses Bertini and Isabel intranuclear cascade models to describe the nuclear interactions mechanism. If the energy falls below the cutoff, the particle transport needs to be performed by the models in MCNP, which are based on ENDF/B cross section libraries; 4) **MCNPX,** released in 1999, is a newly merged code that combines the theoretical models of the LAI-IET Code System with the general features of the MCNP to provide a fully-coupled treatment of the transport problem (Hughes et al. 1997). The code, which is currently only available for UNIX platform, expands the capabilities of MCNP by increasing the set of transportable particles (such as protons). Experience with the beta version shows that MCNPX promises to be a very versatile Monte Carlo code. Together, these codes represent the state-of-the-art in terms of the radiation physics cross-section data and physical models involving photons, electrons, neutrons, and protons. E-mail groups focused on these codes include EGS4-L@mailbox.slac.stanford.edu, mcnp-forum@lanl.gov, and lcs-forum@lanl.gov.

The next section of the article details the development of a new image-based whole-body model from images obtained from National Library of Medicine's Visible Human Project and the procedures to adopt the model into EGS4, MCNP4B, and MCNPX.

MATERIALS AND METHODS

Original images

The quality of original image data for constructing a whole-body model is crucial. At an early stage of our project, several unique sets of whole-body CT/MR/color photographic images from the National Library of Medicine's (NLM) Visible Human Project (VHP) became available (http://www.nlm.nih.gov/research/visible). The ambitious goal of the VHP, which was conceived in 1988 and initiated in 1991, was to build the most detailed digital image library about the anatomies of an adult male and an adult female. VHP is the result of a recommendation from the visionary NLM Board of Regents who foresaw an increasing demand for electronically represented images in clinical medicine and biomedical research (NLM 1990; Ackerman 1995).

Cadavers that were considered "normal" and representative of a large population were evaluated. The donated body of a recently executed 38-y-old male from Texas was the first specimen to be selected for VHP. Later, a 58-y-old female cadaver was also obtained. To ensure the applicability, it was decided that the image data needed to be documented in several common formats used by radiologists and other physicians. Eventually, four modalities were used: traditional x rays and CT scans to optimally visualize bone, MRI for soft tissue, and color photographs for definitive resolution. The color photographs, which had the finest resolution, were used to provide a standard for comparison. Fig. 2 shows the Visible Human Male data set consisting of MRI, CT and color anatomical photographs.

Fig. 2. Images from the Visible Human Project: (Left) Transversal color photography at 2,048 X 1,216 pixel resolution; (Middle) CT images at 512 X 512 pixel resolution; and (Right) MR images at 256 X 256 pixel resolution.

Generally, image format consists of many pixels (picture elements), as shown in Fig. 3, each representing a tissue volume in a 2-D plane. The 3-D volume of the tissue is called a voxel (volume element), and it is determined by multiplying the pixel size by the thickness of an image slice (Bushong 1997). Unlike mathematical whole-body models, an image-based model (also called voxel or tomographic model) contains a huge number of
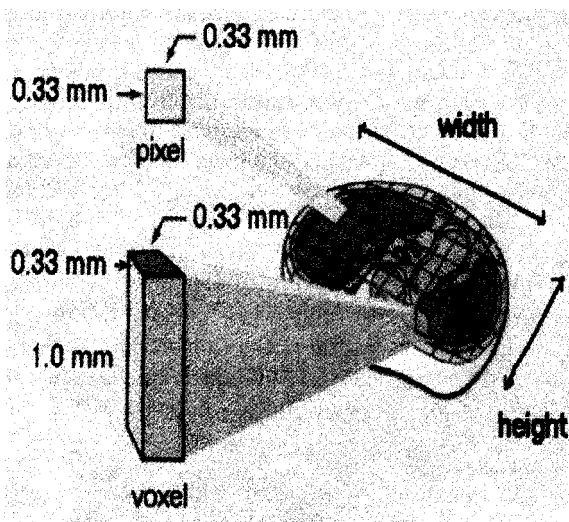
Fig. 3. (a) Illustration of a pixel and a voxel. A whole-body model is made of a huge number of tiny voxels; (b) Original Visible Man obtained from a 38-y-old male cadaver, 186 cm in height and 90 kg in weight. The pixel resolution is 0.33 mm X 0.33 mm at slice thickness of 1 mm. The whole-body image contains 2,048 X 1,216 X 1,871 = 4.7 billion voxels; (c) Original images of the Visible Woman from a 59-y-old female cadaver, 167 cm in height and 72 kg in weight. The pixel resolution is 0.33 mm X 0.33 mm at slice thickness of 0.33 mm. The whole-body image contains 2,048 X 1,216 X 1,871 X 3 = 14.1 billion voxels.

tiny cubes grouped to represent each anatomical structure. Transversal MRI images of the head and neck and longitudinal sections of the rest of the body were obtained at 4 mm intervals. The MRI images are 256 pixel X 256 pixel resolution. Each pixel has 12 bits of gray tone resolution. The voxel size for MRI data (torso portion) set is 1.88 mm X 1.88 mm X 4 mm. The CT data consists of transversal CT scans of the entire body taken at l-mm intervals at a resolution of 5 12 pixels X 512 pixels where each pixel is made up of 12 bits of gray tone. The voxel size for the CT data set (torso portion) is 0.94 mm X 0.94 mm X 1 mm. The transversal anatomical photographs for both male and female cadavers are 2,048 pixels by 1,216 pixels where each pixel is defined by 24 bits of color. The anatomical photographs are at l-mm-thick slices for the male cadaver and 0.33 mm for the female. There are a total of 1,871 slices CT and anatomical photographs (male), respectively. The transversal anatomical images were obtained by photographing the top surface of the body block after removal of (by shaving) each successive millimeter (0.33 mm for the female) by a cryomacrotome. This color photographic data set for whole-body has a voxel size of 0.33 mm X 0.33 mm X 1 mm for the male (0.33 mm X 0.33 mm X 0.33 mm for the female). Fig. 3 also shows the coronal views constructed from the transverse color images. Since the first public debut on 28 November 1994, VHP images have been available in the public domain (www.nlm.nih.gov/research/visible/). Since then, computer engineers and anatomists, working together, have devoted unprecedented effort to classifying and visualizing the data sets. The Visible Human Male is by far the most complete computerized database of the human body ever assembled (Spitzer and Whitlock 1998). Called "the greatest contribution to anatomy since Vesalius's 1543 publication of De Humani Corporis Fabrica," the VHP data sets are the seeds for a growing medical revolution. Today, scientists worldwide for biomedical sciences and engineering applications are utilizing this national resource for anatomical information (NLM 1998). Based primarily on the color photographic images, a model called Visible Photographic Man, or VIP-Man, has been constructed at Rensselaer for radiation transport studies.

Steps to construct whole-body model

In addition to adopting original VHP images, three more steps had to be completed to construct the VIP-Man: 1) Identify and segment the organs or tissues from the original images; 2) Assign physical properties to organs or tissues; and 3) Implement the anatomical data into a Monte Carlo code, These steps are discussed in detail as follows:

1. The original color photographs for the male had been identified and segmented mostly by manual procedures to yield up to 1,400 structures (Spitzer and Whitlock 1998). Organs or tissues adopted to construct VIP-Man include adrenals, bladder, esophagus, gall bladder, stomach mucosa, heart muscle, kidneys, large intestine, liver, lungs, pancreas, prostate, skeletal components, skin, small intestine, spleen, stomach, testes, thymus, thyroid, etc. Additional automatic and manual imaging processing and segmentation were performed by this group to obtain gray matter, white matter, teeth, skull CSF, stomach mucosa, male breast, eye lenses, and red bone marrow. Traditional image processing techniques were employed to identify tissues based on color separation (for example, redness for red bone marrow). GI track mucosa was realistically represented, except for stomach, where one voxel layer on the inner surface of the wall was used. The male breasts were created by defining a region of skin and soft tissue with appropriate weight. The final list covers "critical" organs or tissues that have been assigned "tissue weighting factors" (ICRP 1990; U.S. NRC 1991). Other organs or tissues are included because of their potential roles in biomedical engineering applications. Once an organ or tissue has been segmented, the associated voxels could be arbitrarily colored for visualization. Fig. 4 shows the images before and after the segmentation, as well as the whole-body 3-D distribution of the red bone marrow. In the mathematical model, the skeleton is not realistic and the red bone marrow is not represented. As a result, the dose to the red bone marrow had always been derived from the dose to the bone assuming each of the bones has a uniform marrow distribution (Reece et al. 1994, Xu et al. 1995; Xu and Reece 1996; Reece and Xu 1997). The only radiosensitive tissue that is not available in VIP-Man is the "bone surface," which is defined as the tissue lining the medullary cavity of a bone (ICRP 1975). At an estimated thickness of 0.01 mm, bone surface will have to be based on images of resolution better than a few microns. Fig. 5 presents views of the 3-D VIP-Man.

2. For engineering applications, organs or tissues of interest have to be related to appropriate physical properties. For radiation protection purposes, the average tissue compositions and densities recommended in ICRP 23 were used to tag each voxel in VIP-Man (ICRP 1975). This step allows the radiation interaction cross section library in a Monte Carlo code to be linked to each voxel for radiation transport simulations. Table 1 compares the organ masses of VIP-Man with the Reference Man by ICRP 23 (1975) and mathematical adult male model by Cristy and Eckerman (1987), all using very similar densities. At more than 103 kg, VIP-Man is fatty, having nearly 30 kg more in fat than the Reference Man. The major organs seem to have much more similar masses than the Reference Man. The body had a slight increase in body volume after it was frozen, causing the weight also to increase. The height of VIP-Man is 186 cm, slightly taller than the Reference Man, which has been recently modified to be 174 cm in height and 73 kg in mass (ICRP 1995). The major organs have fairly similar masses. Technically, VIP-Man can be easily re-scaled by a user if necessary, so that the height and total weight agree even better with the Reference
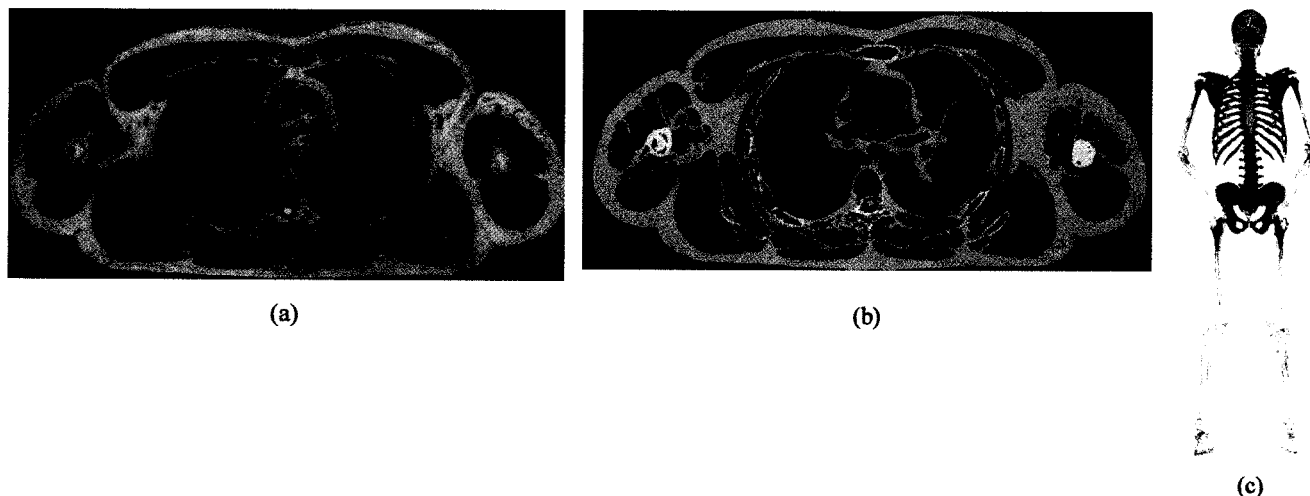
Fig. 4. (a) Original transversal color photograph image (slice No. 1400) at chest level; (b) The same slice after segmentation and classification containing only important organs and tissues; (c) 3-D whole body red bone marrow distribution.

Man. Table 2 lists the mass distributions of red bone marrow and skeleton in VIP-Man in comparison with ICRP 70 Reference Man values (ICRP 1995). As can be seen from Table 2, the mass distribution as segmented for VIP-Man, based on a 38-y-old man, is in remarkable agreement with the ICRP 70 values which were clinically obtained for similar age groups of patients. Table 3 expands the head portion by listing all the tissues that have been included in VIP-Man in comparison with a recently revised MIRD Head/Brain model (Bouchet et al. 1996). There are some noticeable differences in masses, which inevitably will contribute to differences in calculated S-values for internal sources (Snyder et al. 1975; Xu et al. 1999).‡

3. Computers have a limited amount of random accessible memory (RAM). Although today's technologies are much more advanced than a few years ago, the maximum "useable" RAM for a typical PC is often less than 1 GB, seemingly less than the size of VIP-Man containing a total of about 3.7 billion voxels and additional coding. A significant amount of effort was required to reduce the memory burden by using an innovative look-up table (LUT) algorithm. The LUT algorithm was successfully implemented in EGS4, allowing the computer to store only key anatomical and physical data; the details are unfolded from specific tables when needed. The memory saving with the LUT algorithm in VIP-Man/EGS4 is about a factor of 20. On a 450-MHz Pentium II PC of 512 MB RAM, VIP-Man/EGS4 can be run at the

original 0.33 mm X 0.33 mm X 1 mm voxel size. This makes VIP-Man/EGS4 the finest model ever developed for Monte Carlo calculations. MCNP and MCNPX, on the other hand, were designed to be general-purpose codes; therefore, their default code options had to be changed to 'optimize memory. These improvements, however, were not enough, and as a result, the voxel size of VIP-Man/MCNP/X had to be compromised to 4 mm X 4 mm X 4 mm (or about 6 million voxels for the whole body) in order to run it on the same PC. Others have reportedly been able to handle a head model of 65 million voxels in MCNP4A using the ASCI Blue Mountain supercomputer (over 6,000 Parallel CPUs from SGI) at Los Alamos National Laboratory.§‖ Therefore, the original voxel size at 0.33 mm seems to be out of reach for a foreseeable time. Although the resolution for VIP-Man/MCNP/X is limited by the current computer technologies, VIP-Man/MCNP/X is the first whole-body model ever constructed for neutron and proton dose calculations. Although the current running time is more than 10 h due to the size of data, the detailed physics treatments in EGS4, MCNP4B, and MCNPX were not compromised in any way. All of our calculations are being performed on PCs operated under a Linux environment, which is a complete operating system that is similar but not identical to UNIX. The parallel virtual machine (pvm) in Linux enabled us to use multiple CPUs for very time-consuming tasks. Compilers, such as g77, had to be used in EGS4 to

‡ Xu, X. G.; Chao, T. C.; Bozkurt A.; Eckerman, K. F. Voxel-based adult male model using color photographic images from VHP. Invited Presentation at International Workshop on the Development of Human Anatomical Models. Oak Ridge, Tennesseee. September 28-30, 1999.

§ Grooley, J. Voxelized model for MCNP. Private e-mail. 24 May 1999.

‖ McKinney, G. W. Voxelized model for MCNP. Private e-mail. 24 May 1999.

Table 1. Comparison of organ masses for VIP-Man, MIRD Mathematical Phantom, and ICRP 23 Reference Man."

Organs/tissues	VIP-Man (g)	MIRD (g)	ICRP 23 (g)
Adrenals	8.3	16.3	14.0
Bladder (wall)	41.4	47.6	45.0
Bladder (urine)	43.2	211.0	102.0
Brain + nerve	1,574.0	1,420.0	1,429.0
Breast (male)	33.6	403.0	26.0
CSF	265.1	—	121.0
Esophagus (wall)	38.9	—	40.0
Esophagus (lumen)	26.8	—	—
Esophagus (mucosa)	3.5	—	—
Fat	36,326.6	—	17,200.0
Gall bladder (wall)	12.0	10.5	10.0
Gall bladder (bile)	21.0	55.7	60.0
Heart muscle	398.7	316.0	330.0
Kidneys	335.4	299.0	310.0
Lens of eyes	0.54	—	0.4
Liver	1,937.9	1,910.0	1,800.0
Lower large intestine (wall)	290.8	167.0	160.0
Lower large intestine (lumen)	324.2	143.0	135.0
Lower large intestine (mucosa)	35.8	—	—
Lungs	910.5	1,000.0	1,000.0
Muscle	43,002.6	—	28,000.0
Pancreas	82.9	94.3	100.0
Prostate	18.9	—	16.0
Skeleton+RBM	11,244.6	10,000.0	10,000.0
Skin	2,253.4	3,010.0	2,600.0
Small intestine	1,291.8	1,100.0	1,040.0
Spleen	244.0	183.0	180.0
Stomach (wall)	159.5	158.0	150.0
Stomach (content)	324.5	260.0	250.0
Stomach (mucosa)	13.7	—	—
Testes	21 (1)	39.1	35.0
Thymus	11.2	20.9	20.0
Thyroid	27.6	20.7	20.0
Upper large intestine (wall)	461.1	220.0	160.0
Upper large intestine (lumen)	905.7	232.0	135.0
Upper large intestine (mucosa)	63.4	—	—
Other	1,688.0	51,887.7	4,382.0
Total	104,277.2	73,224.8	70,000.0

[a] Reference Man values are from ICRP 23 (1975) and the MIRD model values from Cristy and Eckerman (1987).

accommodate the large integral format.[¶] Since both EGS4 and MCNP4B transport photons and electrons, we were able to "validate" the modeling and Monte Carlo coding by making sure both codes give the same results for VIP-Man (at identical voxel sizes at 4 mm X 4 mm X 4 mm resolution). Fig. 6 compares organ doses from 1-MeV parallel photon beams at anterior-posterior (AP) direction. The calculations took about 50 h for lo-million photons in MCNP and about 25 h for 25-million photons in EGS4. Both codes tracked electrons by different transport algorithms with carefully optimized electron step settings. Results indicated remarkable agreement within the statistical uncertainty between EGS4 and MCNP. More information about benchmarking will be published in a later article.

CONCLUSION

An adult male whole-body model, VIP-Man, has been constructed from the color photographic images of

the famous Visible Human Project. VIP-Man has been adopted into the state-of-the-art Monte Carlo codes, EGS4, MCNP, and MCNPX for radiation transport studies and organ dose calculations involving photons, electrons, neutrons, and protons. To date, VIP-Man represents the world's finest and most complete human anatomical model, containing small tissues, such as skin, GI track mucosa, eye lenses, and red bone marrow, which were not (or not as realistically) represented in the MIRD-based mathematical models and other image-based models. This is also the first time that an image-based whole-body model was adopted for Monte Carlo calculations involving electrons, neutrons, and protons. These advances are significant in that we now are able to investigate subtle dose variations in relatively small structures from various charged particles. The new capability in multiple particle transport not only provides needed health physics dosimetric data but also opens doors for applications in radiotherapy, Compared to MIRD-based mathematical models, VIP-Man is realistic and contains much more anatomical information. The detailed procedure for constructing the image-based models presented in this article should help allow readers to develop their own models in the future.

¶ Chao, T. C.; Bozkurt, A.; Xu, X. G. Development and validation of a specialized Monte Carlo code for voxelized whole body model from very large segmented images. In preparation.

Table 2. Comparison of skeleton and red bone marrow mass distributions from VIP-Man and ICRP 70 (1995) Reference Man.

Bone structure	Red bone marrow		Skeleton (w/marrow)	
	VIP-Man (g)	ICRP 70 Ref. Man (g)	VIP-Man (g)	ICRP 70 Ref. Man (g)
Cranium	48.21	88.92	876.43	1,239.00
Mandible	2.00	9.36	89.14	126.00
Scapulae	46.43	32.76	319.24	378.00
Clavicles	13.41	9.36	102.68	84.00
Sternum	43.13	36.27	117.00	126.00
Ribs	160.80	188.37	728.34	735.00
Cervical vertebrae	22.87	45.63	155.85	
Thoracic vertebrae	145.06	188.37	563.28	1,995.00
Lumbar vertebrae	135.09	143.91	470.22	
Sacrum	110.07	115.83	303.16	
Innominate	315.93	204.75	1,071.43	1,113.00
Femora	41.37	78.39	2,027.67	1,606.50
Tibiae	0.78	—	1,376.93	1,186.50
Other foot	2.01	—	768.96	661.50
Humeri	37.09	26.91	647.61	556.50
Radii and Ulane	2.08	—	379.68	378.00
Other hand bone	1.11	—	244.64	241.50
Other	1.14	1.17	21.01	73.50
Total	1,128.57	1,170.00	10,263.27	10,500.00

Table 3. Comparison of tissues in the head/brain for VIP-Man and recently revised MIRD model (Bouchet 1996).

Tissue/organ	VIP-Man			Revised MIRD head/brain Model		
	Mass (g)	Volume (cm³)	Density (g cm⁻³)	Mass (g)	Volume (cm³)	Density (g cm⁻³)
Caudate nuclei	8.95	8.60	1.04	10.50	10.10	1.04
Cerebellum	122.69	117.97	1.04	139.10	133.75	1.04
Cerebral cortex	681.37	656.11	1.04	622.40	598.46	1.04
Cranial CSF	97.75	94.90	1.03	56.90	54.71	1.04
Cranium	841.44	568.54	1.48	364.60	260.43	1.40
Eyes	14.91	14.48	1.03	15.20	14.62	1.04
Lentiform nuclei	13.41	12.53	1.07	19.40	18.65	1.04
Mandible	86.22	58.26	1.48	170.50	121.79	1.40
Teeth	40.51	19.29	2.10	31.20	22.29	1.40
Thalami	8.07	7.76	1.04	15.70	15.10	1.04
Thyroid	27.56	26.25	1.05	19.90	19.13	1.04
White matter	440.49	422.21	1.04	639.20	614.62	1.04
Lateral ventricle	7.08	6.87	1.03	20.10	19.33	1.04
Corpus callosum	16.92	16.27	1.04	—	—	—
Pons and middle cerebellar peduncle	24.57	23.62	1.04	—	—	—
Fronix	2.22	2.14	1.04	—	—	—
Optic chiasma	0.33	0.32	1.04	—	—	—
Vestibulocochlear	0.07	0.06	1.04	—	—	—
Optic nerve	1.75	1.68	1.04	—	—	—
Lens of eyes	0.54	0.49	1.10	—	—	—

It is perhaps important to note that there are Monte Carlo photon transport codes that lack the capability of transporting electrons. In these codes, secondary electrons from photon interactions have to be assumed to deposit their energies at the interaction sites (i.e., kerma approximation) (ICRP 1996). Kerma approximation is valid only when charged particle equilibrium is established, for example, in a large volume of tissue for mean absorbed dose calculations (Attix 1986). Therefore, high energy photons incident on relatively shallow tissues described by tiny voxels (such as skin, eye lenses or gonads) or at a boundary of tissues having different densities (e.g., bone and lung) would be problematic without tracking secondary electrons. In the case of neutron transport, kerma approximation (i.e., without tracking the recoil protons) should also be practiced with care. This is an important issue that should be kept in mind when comparing dose results obtained from different Monte Carlo codes. A standard procedure for comparing Monte Carlo calculations should also be developed, taking into account of the voxelized small geometries.

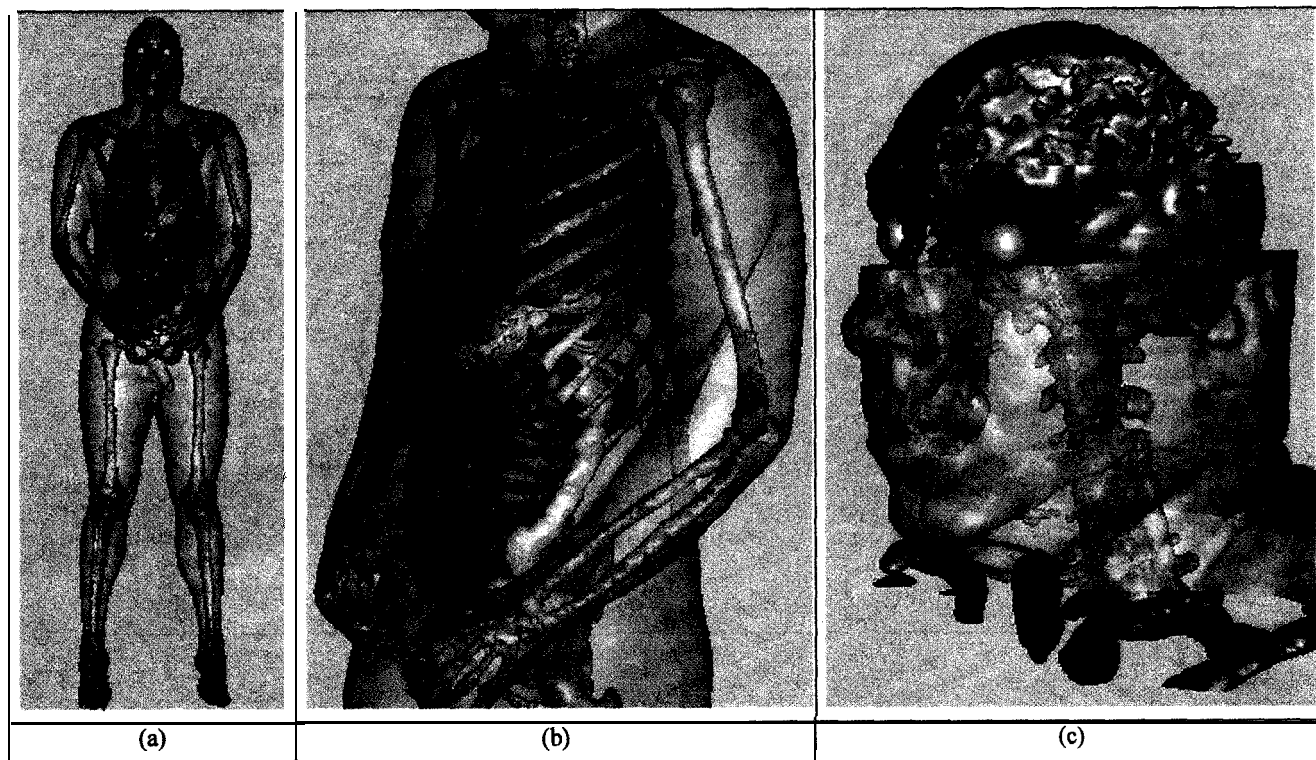VIP-Man is being used to evaluate and compare some of

Fig. 5. VIP-Man in 3-D views showing (a) whole-body skin and skeletal structure; (b) details of internal organs with lungs in red, stomach in gold, upper large intestine in purple, kidney in red, liver in maroon, lower large intestine in brown, etc.; (c) details of the head and brain containing skull in gold, white matter in white, gray matter in gray, nerve in blue, spinal cord in gold, thyroid in red, and skin in white, etc. Visualization Toolkit was used in the surface rendering of the voxelized images (Schroeder et al. 1997).
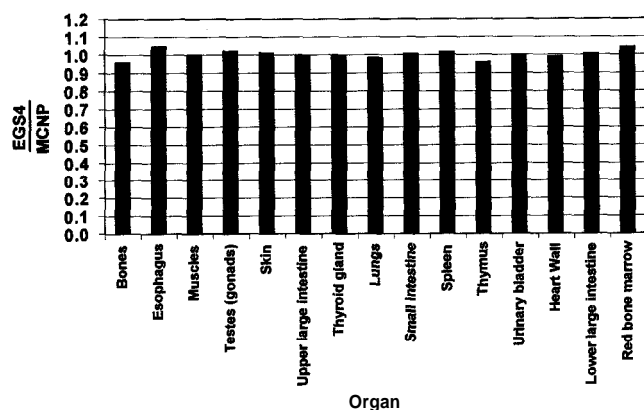
Fig. 6. Comparison of organ doses for VIP-Man using EGS4 and MCNP4B for 1-MeV parallel photon beams at AP direction.

the most important dosimetric quantities for external and internal sources under standard irradiation conditions that have been studied in the past with other models. For more information about this project, please contact the authors or visit http://www.rpi.edu/dept/radsafe/public_html/. Copies of papers and presentations about VP-Man are also available from the Web site. A series of papers, with

interested collaborators, are expected to document all these studies, including results for doses to some of the never-before-modeled organs or tissues. Meanwhile, it should be noted that well-defined MIRD models, although not realistic, have the advantage of being relatively easy to adopt for Monte Carlo calculation and for standardization. This kind of model, however, can be made more anatomically accurate by adopting the data available from VIP-Man and other image-based models. At the present time, it is urgent to fully understand the dosimetric differences between the two types of models. For the purposes of setting radiation protection standards, it may be possible to eventually bridge these two types of models, leading to a new generation of hybrid "standard' model(s) that will be acceptable to the radiation protection community. Such a new generation of models for radiation protection should be realistic enough to accurately represent major radiosensitive tissues and organs, and flexible enough to represent different populations by scaling. Computers are going to be so powerful that very complex models can be handled without a problem. No matter what will happen, however, it is certain that health physics dosimetry will be more realistic and accurate because of these image-based models and the state-of-the-art Monte Carlo techniques. It is anticipated that, for situations involving high occupational radiation exposures (for example, when people travel to the space station on a

daily basis in the future), person-specific dosimetry can be done using images (such as MRI) coupled with rapid segmentation tools and well established Monte Carlo procedures.

VIP-Man also has wide applications in clinical radiotherapy, where highly precise treatment plans have to be verified and optimized with a standard patient dosimetric model (Aldridge et al. 1999). Fundamentally, VIP-Man is digital and it can be easily adopted for applications beyond radiation transport by coupling with physical properties that are electrical, thermal, chemical, mechanical, or biological. When these become technically possible in the future, the reality of "virtual digital human" for every citizen in the "digital society" will be within reach.

REFERENCES

Ackerman, M. J. Accessing the visible human project. D-lib Magazine: The magazine of the digital library forum. 1995. http://www.dlib.org/dlib/october95/10ackerman.html.

Aldridge, J. S.; Rechwerdt, P. J.; Rockie, T. R. A proposal for a standard electronic anthropomorphic phantom for radiotherapy. Med. Phys. 26:1901–1903; 1999.

Attix, F. H. Introduction to radiological physics and radiation dosimetry. New York: John Wiley & Sons; 1986.

Bouchet, L. G.; Bolch, W. E.; Weber, D. A.; Atkins, H. L.; Poston, J. W. Sr. A revised dosimetric model of the adult head and brain. J. Nucl. Med. 37:1226–1236; 1996.

Bushong, S. C. Radiological science for technologists. New York: Mosby-Year Book; 1997.

Cristy, M.; Eckerman, K. F. Specific absorbed fractions of energy at various ages from internal photon sources. Oak Ridge, TN: Oak Ridge National Laboratory; Report No. ORNL/TM-8381/V1; 1987.

Hammersley, J. M.; Handscomb, D. C. Monte Carlo methods. London: Methuen; 1964.

Hartmann Siantar, C. L.; Bergstrom, P. M.; Chandler, W. P.; Chase, L.; Cox, L. J.; Daly, T. P.; Garrett, D.; Homstein, S. M.; House, R. K.; Moses, E. I.; Patterson, R. W.; Rathkopf, J. A.; Schach von Wittenau, A. Lawrence Livermore National Laboratory's PEREGRINE Project. Livermore, CA: LLNL; Report No. UCRL-JC-126732; 1997.

Hendricks, J. S. MCNP4B, LANL memorandum. Los Alamos, MN: Los Alamos National Laboratory; 1997.

Hickman, D. P.; Firpo, M. Magnetic resonance image phantom. Livermore, CA: Lawrence Livermore National Laboratory; UCRL-MA-118455; 1997.

Hughes, H. G.; Prael, R. E.; Little, R. C. MCNPX-The LAHET/MCNP Code Merger. Los Alamos, NM: Los Alamos National Laboratory; XTM-RN(U) 97-012; 1997.

ICRP. Report of the task group on Reference Man. Oxford: Pergamon Press; ICRP Publication 23; 1975.

ICRP. Limits for intake of radionuclides by workers. Oxford: Pergamon Press; ICRP Publication 30; 1979.

ICRP. Data for use in protection against external radiation. Oxford: Pergamon Press; ICRP Publication 51; 1987.

ICRP. Recommendations of the International Commission on Radiological Protection. Oxford: Pergamon Press; ICRP Publication 60; 1990.

ICRP. Basic anatomical and physiological data for use in radiological protection: the skeleton. Oxford: Pergamon Press; Ann. ICRP 25(2), ICRP Publication 70; 1995.

ICRP. Conversion coefficients for use in radiological protection against external radiation. Oxford: Pergamon Press; ICRP Publication 74; 1996.

ICRU. Phantoms and computational models in therapy, diagnosis and protection. Bethesda, MD: International Commission on Radiation Units and Measurements; ICRU Report 48; 1992.

ICRU. Conversion coefficients for use in radiological protection against external radiation. Bethesda, MD: International Commission on Radiation Units and Measurements; ICRU Report 57; 1998.

Jones, D. G. A realistic anthropomorphic phantom for calculating organ doses arising from external photon irradiation. Radiat. Prot. Dosim. 72:21–29; 1997.

Kramer, R.; Zankl, M.; Williams, G.; Drexler, G. The calculation of dose from external photon exposures using reference human phantoms and Monte-Carlo methods, Part 1: The male (ADAM) and female (EVA) adult mathematical phantoms. Munchen: Gesellschaft fur Strahlen-und Umweltforschung mbH; GSF Bericht S-885; 1982.

National Library of Medicine, U.6. Board of Regents. Electronic imaging: Report of the Board of Regents. Bethesda, MD: National Library of Medicine; NIH Publication 90-2197; 1990.

National Library of Medicine. Proceedings of the Second Visible Human Project Conference, October 1-2. Bethesda, MD: National Library of Medicine; 1998.

Nelson, W. R.; Hirayama, H.; Rogers, D. W. 0. The EGS4 code system. Stanford, CA: Stanford Linear Accelerator Center; SLAC-265-UC-32; 1985.

Petoussi-Henβ, N.; Zankl, M. Voxel anthropomorphic models as a tool for internal dosimetry. Radiat. Prot. Dosim. 79:415–418; 1998.

Prael, R. E.; Lichtenstein, H. User guide to LCS: The LAHET code system. Los Alamos, NM: Los Alamos National Laboratory; LA-UR-893014; 1989.

Reece, W. D.; Poston, J. W.; Xu, X. G. Determining the effective dose equivalent for external photons: Calculational results for beam and point-sources. Radiat. Prot. Dosim. 55:5–21; 1994.

Reece, W. D.; Xu, X. G. Determining effective dose equivalent for external photon radiation: Assessing effective dose equivalent from personal dosemeter readings. Radiat. Prot. Dosim. 69: 167-178; 1997.

Schroeder, W.; Martin, K.; Lorensen, B. The visualization toolki-An object-oriented approach to 3D graphics. New Jersey: Prentice Hall; 1997.

Snyder, W. S.; Ford, M. R.; Warner, G. G.; Fisher H. L., Jr. Estimates of absorbed fractions for monoenergetic photon source uniformly distributed in various organs of a heterogeneous phantom. Medical Internal Radiation Dose Committee (MIRD) Pamphlet No. 5, Supplement No. 3. J. Nuclear Med. 10. New York: Society of Nuclear Medicine; 1969.

Snyder, W. S.; Ford, M. R.; Warner, G. G.; Watson, S. B. "S," absorbed dose per unit cumulated activity for selected radionuclides and organs. New York, NY: The Society of Nuclear Medicine; Medical Internal Radiation Dose Committee (MIRD) Pamphlet No. 11; 1975.

Snyder, W. S.; Ford, M. R.; Warner, G. G.; Fisher H. L., Jr. Estimates of absorbed fractions for monoenergetic photon source uniformly distributed in various organs of a heterogeneous phantom. New York, NY: The Society of Nuclear Medicine; Medical Internal Radiation Dose Committee (MIRD) Pamphlet No. 5, Revised; 1978.

Spitzer, V. M.; Whitlock, D. G. Atlas of the visible human male. Sudbury, MA: Jones and Bartlett Publishers; 1998.

U.S. Nuclear Regulatory Commission. Title 10 Part 20 of the Code of Federal Regulations: Standards for protection against radiation. Washington, DC: U.S. NRC; 1991.

Xu, X. G.; Chao, T. C.; Bozkurt, A.; Eckerman, K. F. Development of realistic body models for organ dose calculations. Health Phys. S76:S160; 1999.

Xu, X. G.; Reece, W. D. Sex-specific tissue weighting factors for effective dose equivalent calculations. Health Phys. 70:81–86; 1996.

Xu, X. G.; Reece, W. D.; Poston, J. W. A study of the angular dependence problem in effective dose equivalent assessment. Health Phys. 68:214–224; 1995.

Zubal, I. G.; Harrel, C. R.; Smith, E. 0.; Rattner, Z.; Gindi, G.; Hoffer, P. B. Computerized three-dimensional segmented human anatomy. Med. Phys. 21:299–302; 1994.

■■